

Developmental Anatomy of the Anther in Red Dragon Fruit (*Hylocereus polyrhizus* Britton & Rose)

Utaminingsih¹, Sulhan Etfanti², Maryani^{3*}

^{1,2,3}Department of Biology Tropica, Faculty of Biology, Universitas Gadjah Mada

Abstract

The anatomical development of reproductive organs is critical for understanding reproductive success in flowering plants. In *Hylocereus polyrhizus* (red dragon fruit), pollen viability and anther maturation strongly influence fruit set and breeding success. However, despite the crop's increasing economic importance, detailed anatomical studies of anther development remain limited. This study aimed to characterize the anatomical features and developmental stages of the anther to clarify the mechanisms underlying pollen formation and maturation. Flower buds were sampled at five developmental stages (stages 1–5) and examined histologically using paraffin embedding and safranin staining. Anther length increased progressively by 96% from stages 1 to 4 and then plateaued prior to anthesis, indicating that anther growth ceased before pollen maturation. The anther wall exhibited a typical dicotyledonous structure, consisting of the epidermis, endothecium, middle layer, and tapetum. During early development, archesporial cells differentiated into primary parietal and sporogenous cells, followed by the formation of secondary parietal and sporogenous layers. The endothecium developed characteristic fibrous thickenings, while the binucleate, secretory tapetum supplied nutrients to developing microspores and degenerated at maturity. Microsporogenesis progressed from microspore mother cells to tetrads and free microspores, culminating in tricellular pollen grains at anthesis. These findings indicate that anther development in *H. polyrhizus* follows the typical dicotyledonous pattern, with key features such as a secretory tapetum and a fibrous endothecium. The results provide essential anatomical insights to support breeding programs, artificial pollination strategies, and reproductive biology research in this economically important cactus species.

Keywords: anatomy, anther, development, *Hylocereus polyrhizus*, microsporogenesis

Introduction

Hylocereus polyrhizus, commonly known as red-fleshed dragon fruit, is a member of the Cactaceae family with increasing commercial importance due to its nutritional value, distinctive fruit characteristics, and ornamental appeal. Understanding the reproductive biology

of this species, particularly the development of male (anther) and female (ovule) structures, is crucial for improving pollination efficiency, refining breeding strategies, and optimizing fruit production (Cho, 2021; Kriswiyanti, 2013).

The flowers of *H. polyrhizus* exhibit nocturnal anthesis, numerous stamens,

*Corresponding Author: Utaminingsih, Email: utaminingsih@ugm.ac.id. Sulhan Etfanti, Maryani., Jl. Teknik Selatan, Sekip Utara, Bulaksumur Yogyakarta 55281

a tubular floral structure, and approach herkogamy (spatial separation between the stigma and anthers), which promotes cross-pollination and reduces self-fertilization (Cho & Ding, 2022). Combined with a dry-type stigma, these traits contribute to a self-incompatibility system, making cross-pollination, either by nocturnal pollinators such as bats and hawkmoths or through manual intervention, essential for achieving high fruit set (Cho, 2021; Cho & Ding, 2022).

Anther development in *H. polyrhizus* follows a typical dicotyledonous pattern, beginning with the differentiation of primary parietal and sporogenous cells and progressing through the formation of secondary sporogenous cells, microspore tetrads, and ultimately mature tricellular pollen grains. Ovule development proceeds through nucellus and integument differentiation, megasporogenesis, and megagametogenesis, culminating in the formation of an eight-nucleate embryo sac (Etfanti & Suharyanto, 2018). Documenting these stages provides valuable insight into reproductive timing, pollen viability, and potential intervention points for controlled pollination.

Beyond natural reproductive processes, anther culture experiments have demonstrated androgenic callus formation in *H. polyrhizus*, although successful plant regeneration remains limited (Chávez-Vela et al., 2008). Such *in vitro* approaches, when integrated with detailed knowledge of floral organ development, may accelerate breeding programs and facilitate the production of homozygous lines (Tel-Zur et al., 2022).

Although several studies have examined the general floral anatomy of *H. polyrhizus*, detailed information on stage-specific stamen development remains limited. Therefore, the present study aimed to describe the developmental anatomy of the anther in *H. polyrhizus* through histological and microscopic analyses. A clearer understanding of anther development is expected to support improvements in artificial pollination techniques, enhance breeding efficiency, and provide a foundation for future biotechnological applications in this economically important species.

Research Methods

Sample collection

Samples were collected from an orchard located in the Lemponsari area, Ngaglik, Sleman, Yogyakarta. Sampling was conducted at various stages of flower development. The transition from bud initiation to full anthesis in *H. polyrhizus* flowers took approximately 20 days. *H. polyrhizus* flower buds were classified into five developmental stages based on bud size and morphological characteristics. Sampling was performed with three replications for each developmental stage. The developmental stages of the flower buds are presented in Table 1.

Anatomical Preparation

Anatomical preparation followed the method described by Ruzin (1999). Anther samples were fixed in FAA solution (formalin : glacial acetic acid : 70% ethanol = 5 : 5 : 90) for 24 hours. The fixative was then discarded and replaced sequentially with 70%, 80%, 95%, and 100% ethanol, each applied

twice for 30 minutes per step. Dehydration was followed by dealcoholization using graded mixtures of ethanol and xylol (3:1, 1:1, and 1:3), and subsequently two changes of pure xylol, each for 30 minutes. Samples were then infiltrated with a xylol-paraffin mixture (1:9) at 57°C for 24 hours, followed by infiltration in pure paraffin for an additional 24 hours at the same temperature. A final change to fresh pure paraffin was conducted prior to blocking.

Paraffin blocks were sectioned transversely using a rotary microtome at a thickness of 16 µm. Sections were mounted on glass slides coated with glycerin-albumin and placed on a hot plate at 45°C to flatten the paraffin ribbons. Staining was performed using 1% safranin in 70% ethanol for 1 hour. Following staining, the slides were dehydrated through a graded alcohol-xylol series consisting of 70%, 80%, 95%, and 100% ethanol (each applied twice for 3 minutes), followed by ethanol/xylol mixtures (3:1, 1:1, and 1:3) and two final changes of pure xylol for 1 minute each. Sections were then mounted using Canadian balsam, covered with cover slips, and dried on a hot plate at 45°C until the mounting medium was fully set.

Data Analysis

Qualitative data were obtained from specimens photographed using a Miconos Upgrade Edition Optilab microscope camera. Observations focused on anther anatomical features at different developmental stages, including the epidermis, endothecium, middle layer, and tapetum, as well as

microsporogenesis and microgametogenesis processes involving microsporocytes, microspore tetrads, young microspores, and mature microspores. All qualitative observations were analyzed descriptively. Quantitative measurements were limited to anther length.

Research Results and Discussion

Morphology of Anther Development

Anther length increased across developmental stages (see Table 2 and Figure 1), exhibiting a distinct pattern of growth. From stages 1 to 4, anther length showed a consistent increasing trend, whereas from stages 4 to 5 the increase became minimal, forming a near-horizontal pattern. Overall, anther size increased by approximately 96% from stages 1 to 5, while the increase from stages 4 to 5 was only about 4%. These findings indicate that anther development is directly proportional to its developmental stage. The increase in anther size is driven by an increase in cell number and cell expansion. In addition, anther cells undergo differentiation, resulting in the formation of specialized structures with specific functions. This reflects the fundamental components of development, namely growth, differentiation, and morphogenesis, as described by Srivastava (2002). Growth refers to increases in cell number and size that lead to greater mass. Differentiation involves qualitative changes that distinguish cells from their parent cells and from cells in other organs. Morphogenesis refers to the acquisition of a specific form. Cell division during growth occurs through formative division, which produces cells dissimilar to the parent cell, and

proliferative division, which produces cells similar to the parent cell.

Based on these observations, anther size increased progressively by 24%, 77%, 96%, and ultimately 100% across successive stages. The increase from stages 1 to 4 followed a clear upward trend, while the transition from stages 4 to 5 showed minimal growth. These size changes resulted from coordinated growth and differentiation processes, which were affected by both internal and external factors.

In plant development, cell expansion, division, and differentiation are essential and interconnected processes. Cell expansion occurs as a result of turgor pressure, leading to cell elongation, while cell division involves the formation of new cell walls. Cell differentiation proceeds alongside these processes until cells reach their final form. Continued anther development is also supported by increased nutrient availability. Developmental processes are regulated by external and internal factors. External factors include environmental influences such as xenobiotics, resources, and stressors. Xenobiotics include air pollutants and organic or inorganic toxins, while resources include light, CO₂, water, nitrogen, and phosphorus. Stressors encompass temperature, salinity, and soil pH (Willey, 2016). Internal factors include hormonal regulation and genetic control (Davies, 2010; Pierik, 1997).

Anatomy of Anther Development

This study examined anther development from stages 1 to 5. The anther consisted of four main layers: the epidermis, endothecium, middle layer, and tapetum (see Figure 2). At stage 1,

young anthers containing four microsporangia were observed. The epidermis formed the outermost layer of the anther and consisted of a single layer of cells. Beneath the epidermis were the primary parietal cells, while the sporogenous cells were located internally. Pollen development proceeded through microsporogenesis and microgametogenesis. At this stage, both primary parietal cells and primary sporogenous cells had differentiated (see Figure 2A).

The anther primordium originated from the floral meristem and appeared as a mass of cells containing epidermal cells. According to Bhojwani et al. (2015), epidermal cells divide anticlinally during development. Within the hypodermal layer, certain cells became morphologically distinct; they were larger, exhibited slight radial elongation, and possessed prominent nuclei. These cells are known as archesporial cells. Bhojwani et al. (2015) further reported that archesporial cells are more conspicuous than surrounding cells due to their size and nuclear prominence.

Archesporial cells were divided periclinally to produce two layers: an outer layer known as the primary parietal cells and an inner layer known as the primary sporogenous cells. The primary parietal cells gave rise to the anther wall layers, whereas the primary sporogenous cells developed into secondary sporogenous cells, which subsequently differentiated into microsporocytes. This developmental pattern is consistent with the description by Srivastava et al. (2002),

who stated that both primary parietal and primary sporogenous cells originate from archesporial cells (see Figure 2A).

At stage 2, the epidermis remained clearly visible, and its cells were larger than those of the endothecium and middle layers. The endothecium consisted of a single layer of flattened cells, while the middle layer was composed of two flattened cell layers. The tapetum appeared more intensely stained than the other anther wall layers due to its dense cytoplasmic content. Tapetal cells were binucleate and arranged in two layers. Within the microsporangium, large and conspicuous secondary sporogenous cells were observed, each with a single prominent nucleus that distinguished them from the surrounding anther wall cells (see Figure 2B).

During this stage, primary parietal cells were divided to form outer and inner secondary parietal cells. The outer secondary parietal cells were divided periclinally to form the endothecium and middle layers, while the inner secondary parietal cells were differentiated into tapetal cells. Consequently, the anther wall developed according to the dicotyledonous type. This pattern is consistent with findings by Gotelli et al. (2009), who reported that the anthers of *Pterocactus* (Cactaceae) exhibit dicotyledonous development (see Figure 2B).

The tapetum continued to thicken and remained binucleate. At later stages, the tapetum disappeared as pollen matured, a process attributed to the release of its cytoplasmic contents to nourish developing microspores. Papini et al. (2014) reported that the tapetum plays a primary role in pollen nutrition and in the formation of pollen exine

components. The tapetum in this study was classified as secretory, as it did not disintegrate immediately during microspore development. Similar secretory tapetum types have been reported in several cacti, including *Lobivia rauschii* (Papini et al., 2014) and *Echinocactus phyllanthus* (Almaida, 2010) (see Figure 2B).

At stage 3, the epidermis remained visible but became thinner and began to appear wavy. The endothecium layer increased in size, while the middle layer was no longer distinguishable. Tapetal cells appeared thinner, indicating degeneration, although the tapetum remained secretory. Microspores were observed as solitary units, but their nuclei were not clearly visible (see Figure 2C and Figure 2F).

In stage 4, the epidermis persisted, with deeper grooves that gave it a flattened appearance with tapered tips. The endothecium underwent fibrous thickening. At this stage, the tapetum was no longer present, and the stomium had not yet formed. Solitary microspores were observed, with nuclei located centrally within the cells. This stage marked the completion of microsporogenesis (see Figure 2D and Figure 2G).

The fibrous thickening of the endothecium, often referred to as the fibrous lamina, resulted from tangential and radial expansion of endothelial fibers. This observation is consistent with previous reports indicating that the endothecium widens and thickens inwardly during anther maturation (Strittmatter et al., 2002; Gotelli et al., 2009).

The absence of the middle layer in mature anthers was attributed to compression caused by the expansion of

the endothecium and tapetum during development. Nugroho et al. (2012) reported that the middle layer becomes flattened, compressed, and eventually disappears (see Figure 2B).

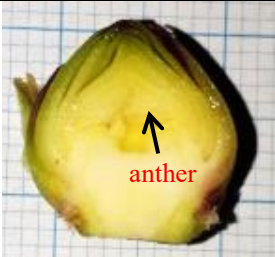
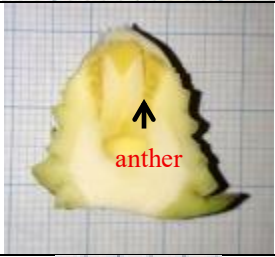
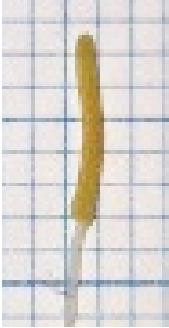

At stage 5, the epidermis remained visible, with grooves becoming more pronounced, giving the appearance of separation. The endothecium exhibited further fibrous thickening, and the stomium became apparent. The stomium was present in each microsporangium and was located near the connective tissue. At this stage, the sporangium opened, marking the transition from microsporogenesis to microgametogenesis. This process involved the formation of male gamete nuclei. Observed microspores at this stage contained one vegetative nucleus and two gamete nuclei. The vegetative nucleus was larger and more rounded, while the gamete nuclei were smaller, flattened, and tapered. Microspores were released from the anther in the tricellular stage (see Figure 2E and Figure 2H).

The final phase of microsporogenesis resulted in the formation of solitary microspores, after which microgametogenesis began. During microgametogenesis, the microspore nucleus underwent the first mitotic division (mitosis I), producing a vegetative nucleus and a generative nucleus located near the cell wall. The generative nucleus subsequently migrated toward the center of the cell and underwent a second mitotic division (mitosis II), producing two gamete nuclei. Together with the vegetative nucleus, these nuclei formed mature pollen grains. The presence of tricellular pollen has been reported in several members of the Cactaceae. For example, *Hylocereus undatus* produces mature tricellular pollen (Wang, 2007) (see Figure 2H). To summarize the stages of anther development, the observations are presented in Table 3.

Table 1.
Stages of flower bud development in H. polyrhizus plants.

Stage	Days Before Anthesis	Characteristic Features
1	17	Flower size was approximately 1 cm; the bud was still small; petals were green with a red tinge and distinct red coloration at the edges and tips.
2	13	Flower size was approximately 5 cm; the bud enlarged; petals were green with red coloration at the edges and a red tinge at the center.
3	9	Flower size was approximately 11 cm; the bud elongated at the base; petals were green with red coloration at the edges and a red tinge at the center.
4	5	Flower size was approximately 21 cm; the bud continued to elongate, and the hypanthium became distinguishable.
5	1	Flower size was approximately 30 cm; the bud reached its maximum size; the flower bud became lighter in color with red coloration at the petal edges.

Table 2.*Anther length at various stages of development.*

Stage	Days Before Anthesis	Anther Morphology	Anther Length (cm)
1	±17		0.05 ± 0.00
2	±13		0.27 ± 0.06
3	±9		0.75 ± 0.05
4	±5		0.92 ± 0.03

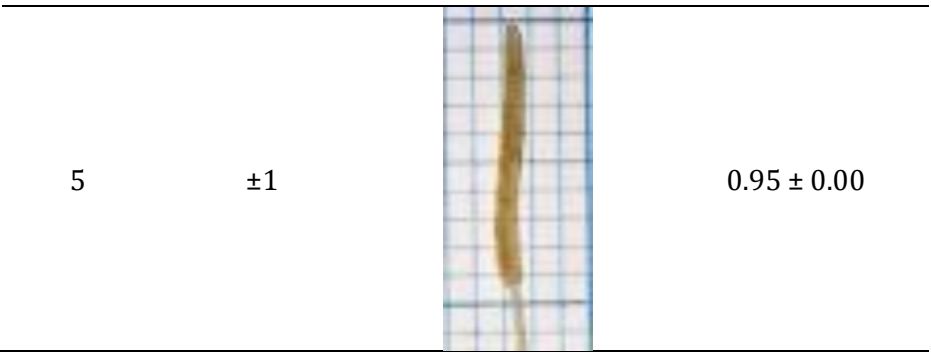


Figure 1
Anther length at various stages of development.

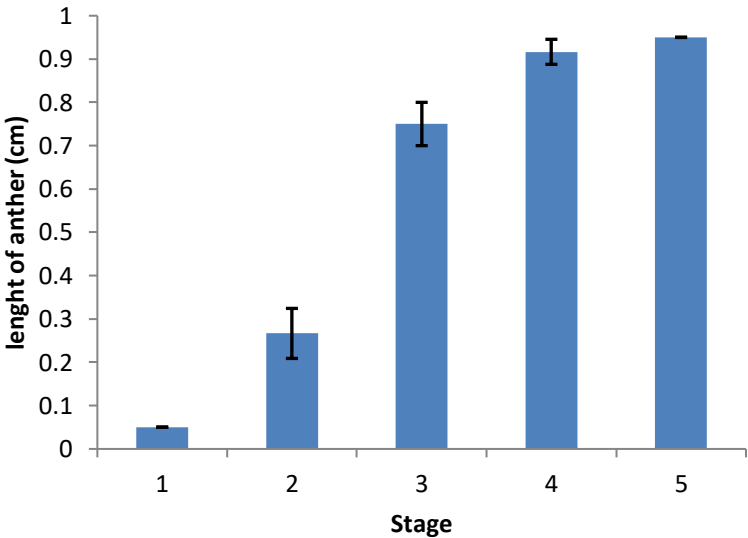


Figure 2.

Cross-sections of the anther of H. polyrhizus flowers at different developmental stages. A = Stage 1; B = Stage 2; C = Stage 3; D = Stage 4; E = Stage 5; F = sporangium containing tetrad spores; G = sporangium containing solitary microspores; H = three-nucleated microspores at Stage 5. Description: 1) primary parietal cell, 2) epidermis, 3) primary sporogenous cell, 4) secondary sporogenous cell, 5) endothecium, 6) middle layer, 7) tapetum, 8) vascular bundle, 9) solitary microspore, 10) microspore nucleus, 11) vegetative nucleus, 12) generative nucleus, 13) stomium, 14) tapetum remnant.

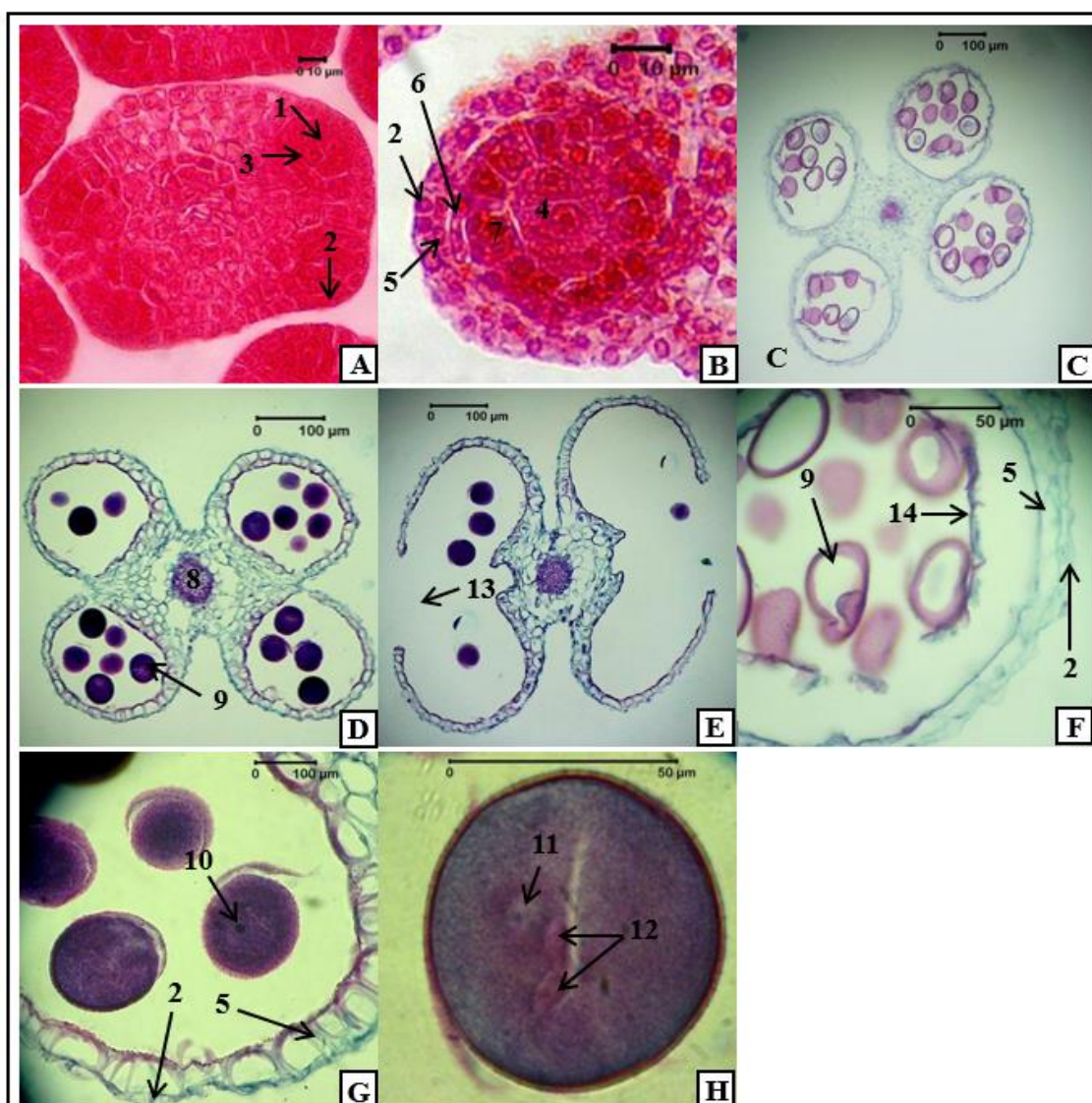


Table 3.

Stages of anther development in H. polyrhizus flowers.

Stage	Days Before Anthesis	Anther Development
1	17	Young anthers contained epidermal cells, primary parietal cells, and primary sporogenous cells.
2	13	Anther size increased by 24%. The anther wall consisted of the epidermis, endothecium, middle layer, and tapetum. Secondary sporogenous cells were present.
3	9	Anther size increased by 77%. The epidermis became flatter, the endothecium thickened, the tapetum persisted, and the middle layer disappeared. Solitary microspores were present.
4	5	Anther size increased by 96%. The epidermis became indented, the endothecium became fibrous, the tapetum degenerated, a stomium formed, and solitary microspores were present.
5	1	Anther size increased by 100%. The stomium ruptured, the microsporangium opened, and microspores were released. Three-nucleated microspores were present.

Anther development in *H. polyrhizus* followed a typical dicotyledonous pattern, progressing from the early differentiation of parietal and sporogenous tissues to anther dehiscence near anthesis. During the early stages (17–13 days before anthesis), young anthers consisted of epidermal, primary parietal, and primary sporogenous cells, which subsequently differentiated into four distinct wall layers, including epidermis, endothecium, middle layer, and tapetum, accompanied by the formation of secondary sporogenous cells. In the intermediate stages (9–5 days before anthesis), the anther enlarged substantially, the endothecium thickened, and the middle layer and tapetum gradually degenerated, while solitary microspores became evident. By one day before anthesis, the stomium ruptured, allowing the release of mature, three-nucleated pollen grains. This developmental sequence highlights the coordinated processes of tissue differentiation and male gametophyte formation and reflects a conserved pattern of anther ontogeny within the Cactaceae.

Conclusion

Anther growth reached its maximum size at stage 4, whereas anatomical maturity occurred at stage 5, coinciding with pollen readiness. The anther wall exhibited a dicotyledonous type. The anther consisted of four microsporangia, which were surrounded by several anther wall layers: the epidermis, endothecium, middle layer, and tapetum. Microspore development progressed through the primary parietal cell stage, secondary sporogenous cell stage, solitary microspore stage, and three-nucleated microspore stage.

Acknowledgment

The authors gratefully acknowledge the Research Directorate of Universitas Gadjah Mada for financial support through the 2016 Lecturer Research Capacity Enhancement Grant.

References

Almeida, O. J. G., Sartori-Paoli, A. A., & Souza, L. A. (2010). Flower morpho-anatomy in

Epiphyllum phyllanthus (Cactaceae). *Revista Mexicana de Biodiversidad*, 81, 65–80.

Bhojwani, S. S., Bhatnagar, S. P., & Dantu, P. K. (2015). *The embryology of angiosperms* (6th ed., pp. 14–65). Vikas Publishing House Pvt Ltd.

Britton, N., & Rose, J. N. (1963). *The Cactaceae: Description and illustrations of plants of the cactus family* (Vols. 1–2, pp. 183–185). Dover.

Chávez-Vela, N. A., Reyes, A., & Tel-Zur, N. (2008). Androgenesis in the vine cacti *Selenicereus* and *Hylocereus*. *Plant Cell, Tissue and Organ Culture*, 96, 191–199. <https://doi.org/10.1007/s11240-008-9475-9>

Cho, J. L. Y. (2021). Floral morphology and pollination process of red-fleshed dragon fruit (*Hylocereus polyrhizus*). *Horticultural Science and Technology*, 39(3), 277–293. <https://doi.org/10.7235/HORT.20210025>

Cho, J. L. Y., & Ding, P. (2022). Floral characteristics of red-fleshed dragon fruit (*Hylocereus polyrhizus*) grown under Malaysian climate. *Acta Horticulturae*, 1342, 143–150. <https://doi.org/10.17660/ActaHortic.2022.1342.20>

Davies, P. J. (2010). *Plant hormones: Biosynthesis, signal transduction, action* (p. 179). Springer Science+Business Media.

Etfanti, S., & Suharyanto, E. (2018). *Perkembangan anatomis bunga buah naga merah (Hylocereus polyrhizus)* [Undergraduate thesis, Universitas Gadjah Mada]. UGM Repository. <https://etd.repository.ugm.ac.id/home/detail/pencarian/153936>

Gotelli, M. M., Scambato, A., Galati, B., & Kiesling, R. (2009). Pollen development and morphology in four species of *Pterocactus* (Cactaceae). *Annales Botanici Fennici*, 46(5), 409–415.

Kriswiyanti, E. (2013). The generative reproductive characteristics of red dragon

fruit (*Hylocereus polyrhizus*). *Jurnal Biologi Udayana*, 16(1), 13–19. <https://ojs.unud.ac.id/index.php/bio/article/view/5702>

Nugroho, L. H., Purnomo, & Sumardi, I. (2012). *Struktur dan perkembangan tumbuhan* (pp. 120–156). Penebar Swadaya.

Papini, A., Mosti, A., & Doorn, W. G. V. (2014). Classical macroautophagy in *Lobivia rauschii* (Cactaceae) and possible plastidial autophagy in *Tillandsia albida* (Bromeliaceae) tapetum cells. *Protoplasma*, 251, 719–725.

Pierik, R. L. M. (1997). *In vitro culture of higher plants* (p. 45). Springer Science+Business Media.

Srivastava, L. M. (2002). *Plant growth and development: Hormones and the environment* (p. 5). Academic Press.

Strittmatter, L. I., Negron-Ortiz, V., & Hickey, R. J. (2002). Subdioecy in *Consolea spinosissima* (Cactaceae): Breeding system and embryological studies. *American Journal of Botany*, 89(9), 1373–1387.

Tel-Zur, N., Ben-Naim, Y., Cisneros, A., & Mizrahi, Y. (2022). Breeding an underutilized fruit crop: A long-term program for *Hylocereus*. *Plants*, 11(12), 1614. <https://doi.org/10.3390/plants11121614>

Willey, N. (2016). *Environmental plant physiology* (p. 8). Garland Science, Taylor & Francis Group.